CEAI, Vol.13, No.1, pp. 62-68, 2011 Printed in Romania

Advantages of Robust Control for Series Load Frequency Controlled Induction Heating Inverters

T. Szelitzky, I. Inoan, D. C. Dumitrache

Technical University of Cluj Napoca,Faculty of Automation and Computer Science
Cluj Napoca, Romania (e-mail:sztibi82@yahoo.com,iuliainoan@yahoo.com, dan.dumitrache@aut.utcluj.ro).

Abstract: The new generation of microcontrollers on 32 bits allows the implementation of fast and complex controlling algorithms, like robust control. In the present paper the advantages of robust control will be presented in comparison with classic PI controller design using root locus method. The frequency controlled series resonant load induction heating inverter model will be presented with uncertainties together with the design approach for computing H_∞ and PI controller. Simulation results will be compared for the same plant using the two controllers.

Keywords: Induction heating, inverter, robust control, root locus design method, frequency control

1. INTRODUCTION

The presence of high speed microcontrollers and DSPs makes available the development of advanced and complex control techniques like: fuzzy control (Tomse, 2007) self tuning PID control (Uchihori, 1995) Lyapunov-Based Frequency-Shift Power Control (Kelemen, 2009) and robust control (Szelitzky, 2010). The present paper proposes the design of a robust controller for frequency controlled series load induction heating inverter.

The advantages of robust control will be presented in comparison with a PI controller tuned using root locus. The controlled plant is a 15kHz 3.5kW power induction heating inverter, heating a 50mm diameter and 70mm long copper bar.

Induction heating is an efficient and clean heating method. The work piece is heated directly through Joule-Lenz effect of the eddy currents induced by a variable electromagnetic field. The electromagnetic field is generated by high frequency alternating current passing the inductor.

To control the output variables of the inverter the following methods was in the past developed (Fujita, 1993):

Varying inverter supply voltage:

controlled rectifier, (by adjusting the firing angles of the thyristors, inverter supply voltage is altered)

DC-DC power supply, (the inverter supply voltage is altered by a variable voltage DC to DC power supply)

Varying through inverter:

pulse width control, (by adjusting the pulse width of the driving signals of the power transistors, inverter output parameters are altered)

frequency control, (the increase or decrease of the switching frequency relative to resonant frequency all output parameters of the inverter are decreased)

phase control, (by adjusting the phase difference between power transistors in diagonal, output parameters of the inverter is controlled)

In our case the frequency control was chosen to adjust the resonant capacitor voltage. The block diagram of the induction heating inverter studied in this paper is presented in figure 1.

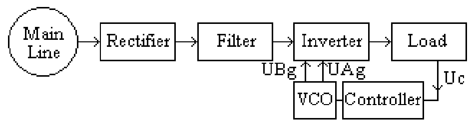

Fig. 1. Block diagram of frequency controlled induction heating inverter.

The ratio between capacitor voltage and supply voltage with respect to switching frequency and resonant frequency ratio can be observed in figure 2. As it can be seen, the further the switching frequency is from the resonant frequency of the load circuit, the capacitor voltage decreases.

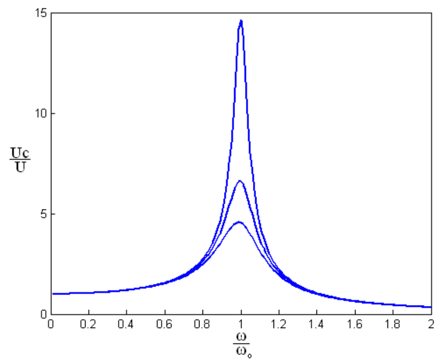

Fig. 2. Capacitor voltage/supply voltage vs frequency/resonant frequency.

The dependency between supply voltage and resonant capacitor voltage is described by the equation (Iordache, 2000):

$$\frac{U_c}{U} = \frac{Q\frac{\omega_0}{\omega}}{\sqrt{1+Q^2\left(\frac{\omega}{\omega_0}-\frac{\omega_0}{\omega}\right)^2}} \quad (1)$$

Where the quality factor has the following form:

$$Q = \frac{\omega_0 L}{R} \quad (2)$$

1.2 Power transistor driving signals

The driving signals of the power transistors for this power control are square waves with 50% duty cycle. In practice we have to choose a dead time which has as effect the reduction of the duty cycle. This dead time has to be taken sufficient long so that the parasitic capacitors of the switches can be charged or discharged (Kazimierczuk, 1995). For the bridge topology (4 transistors) we have the following driving signals.

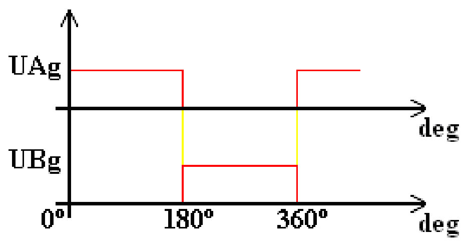

Fig. 3. Ideal transistor driving signals.

The bridge topology has the following electric circuit:

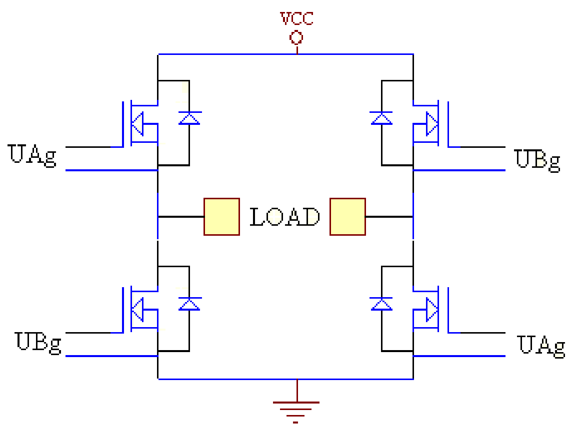

Fig. 4. Bridge topology.

In the series resonant load inverters, the power switches (the transistors) has to be bidirectional for current and unidirectional for voltage, because of phase difference between the resonant voltage and current, there are some time intervals in which power is transferred from the load to the power supply (Dede, 1991).

2. PROCESS DESCRIPTION

The induction heating inverter controlled in the present paper consists of 4 ideal transistors feeding a series resonant load circuit. The load circuit consist of a capacitor, matching transformer and the inductor. The inductor is represented through an ideal coil (R=0) and a resistor. The schematic of the circuit is presented in figure 5. This circuit through simple circuit solving methods can be simplified into RLC series circuit.

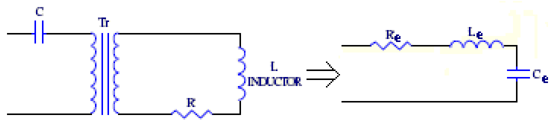

Fig. 5. Resonant circuit.

For the simulations the heated material is chosen copper. This means that the inductivity change is not significant in comparison with resistor value changes. To obtain the values of R and L the following inductor work piece geometry was used:

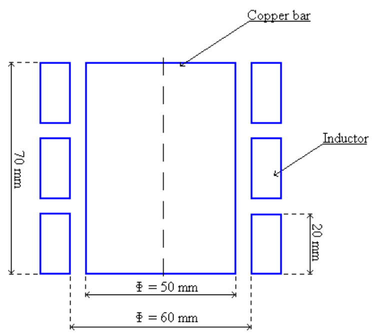

Fig. 6. Inductor geometry.

To estimate the equivalent resistance and inductivity of the inductor-work piece, FEMM 4.2 was used a finite element methods program. The equivalent resistors value was calculated to vary between 0.25Ω and 0.66Ω. The 0.25Ω is for the inductor with copper at room temperature and 0.66Ω is considered for inductor full with molten copper.

Resistor and quality factor dependency in function of temperature can be observed in figure 7.

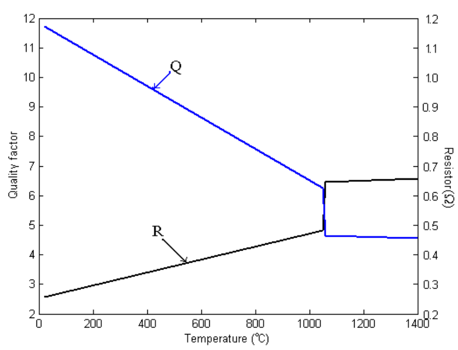

Fig. 7. Quality factor and equivalent resistor value vs. temperature.

The effect of increase of resistor value with temperature is the decrease of the quality factor of the resonant circuit. For the inductor with copper at room temperature the quality factor is 11.7 and for the inductor full with molten copper the circuit's quality factor is 4.6.

3. H$_\infty$ ROBUST CONTROL

The H$_\infty$ robust controller synthesis consist of finding such a controller K which keeps the infinity norm of the output z of the plant G under a given value, while achieving robust stability and performance in presence of uncertainty (Toivonen, 1998) (Damen, 2002).

Let's consider the following representation of the plant G:

$$\begin{aligned} x(t) &= Ax(t) + B_1v(t) + B_2u(t) \\ z(t) &= C_1x(t) + D_{11}v(t) + D_{12}u(t) \\ y(t) &= C_2x(t) + D_{21}v(t) + D_{22}u(t) \end{aligned} \tag{3}$$

Where G can be written in form:

$$G = \left(\begin{array}{c|cc} A & B_1 & B_2 \\ \hline C_1 & D_{11} & D_{12} \\ C_2 & D_{21} & D_{22} \end{array} \right) \tag{4}$$

The aim is to find a controller which stabilizes the system and minimizes the H$_\infty$ norm of the lower linear fractional transformation F(G,K)(Doyle, 1989).

$$F(G,K) = G_{11} + G_{12}(I - KG_{22})^{-1} KG_{21} \tag{5}$$

$$J_\infty(K) = \|F(G,K)\|_\infty < \gamma \tag{6}$$

We introduce the following Hamiltonian matrices:

$$H_\infty = \begin{bmatrix} A & \gamma^{-2}B_1B_1^T - B_2B_2^T \\ -C_1^TC_1 & -A^T \end{bmatrix} \tag{7}$$

$$J_\infty = \begin{bmatrix} A^T & \gamma^{-2}C_1C_1^T - C_2C_2^T \\ -B_1^TB_1 & -A \end{bmatrix} \tag{8}$$

If (A,B1) and (A,B2) is stabilisable, (C1,A) and (C2,A) is detectable, $C_1^TD_{12}$ and $B_1D_{21}^T$ equals 0 while $D_{12}^TD_{12} = I$, $D_{21}D_{21}^T = I$ exists and internally stabilizing controller if and only if:

$$X_\infty = Ric(H_\infty) \geq 0 \tag{9}$$

$$Y_\infty = Ric(J_\infty) \geq 0 \tag{10}$$

$$\rho(X_\infty Y_\infty) < \gamma^2 \tag{11}$$

The controller can be calculated using (Sanchez-Pena, 1998):

$$K_{(s)} = F_l(M_\infty, Q) \tag{12}$$

where:

$$M_\infty = \begin{bmatrix} A_\infty & -Z_\infty L_\infty & Z_\infty B_2 \\ F_\infty & 0 & I \\ -C2 & I & 0 \end{bmatrix} \tag{13}$$

$$A_\infty = A + \gamma^{-2}B_1B_1^TX_\infty + B_2F_\infty + Z_\infty L_\infty C_2 \tag{14}$$

$$F_\infty = -B_2^TX_\infty \tag{15}$$

$$L_\infty = -Y_\infty C_2^T \tag{16}$$

$$Z_\infty = \left(I - \gamma^{-2}Y_\infty X_\infty\right)^{-1} \tag{17}$$

$$\|Q\|_\infty < \gamma \tag{18}$$

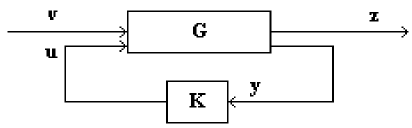

Fig. 8. General Robust feedback control system.

Were:

x- state vector, v- input vector, u- control input vector

y- measurement vector, z- output vector

4. ROBUST CONTROL OF AN INDUCTION HEATING INVERTER

The first step in the design procedure of the H$_\infty$ controller is the creation of the plant model with uncertainties of the voltage source frequency controlled induction heating inverter.

To obtain the state space model of the inverter, the resonant circuit was analyzes using Fourier transform (Tomse, 2004). The following state space equations resulted:

$$\begin{bmatrix} \dot{U}cs \\ \dot{I}s \\ \dot{U}cc \\ \dot{I}c \end{bmatrix} = \begin{bmatrix} 0 & 1/C & \omega & 0 \\ -1/L & -R/L & 0 & \omega \\ -\omega & 0 & 0 & 1/C \\ 0 & -\omega & -1/L & -R/L \end{bmatrix} \begin{bmatrix} Ucs \\ Is \\ Ucc \\ Ic \end{bmatrix} + \begin{bmatrix} 0 \\ -4/\pi/L \\ 0 \\ 0 \end{bmatrix} Udc$$

$$Y = \sqrt{U^2cc + U^2cs} \tag{19}$$

We linearized the system around a working point and obtained the following model of the resonant load frequency controlled inverter:

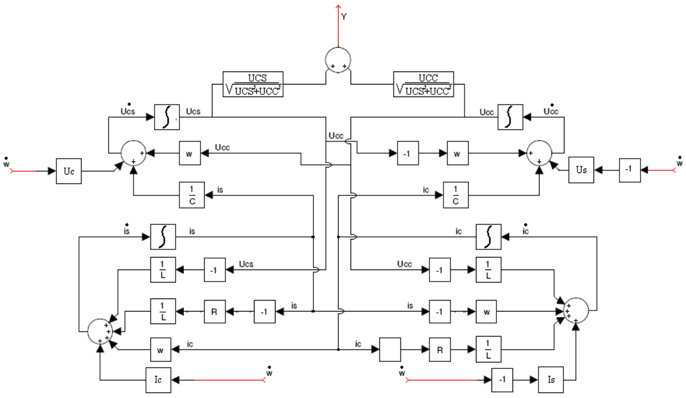

Fig. 9. Linearized system model

The blocks containing R were changed with uncertainties:

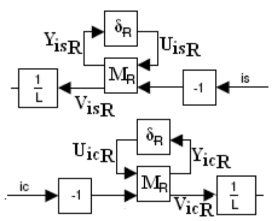

Fig. 10. Introduction of uncertainties

For this particular application the following plant model with uncertainties resulted:

$$G=\begin{bmatrix} 0 & \frac{1}{C} & \omega & 0 & 0 & 0 & Uc_{\cos} \\ -\frac{1}{L} & -\frac{\overline{R}}{L} & 0 & \omega & \frac{\Pr}{L} & 0 & I_{\cos} \\ -\omega & 0 & 0 & \frac{1}{C} & 0 & 0 & -Uc_{\sin} \\ 0 & -\omega & -\frac{1}{L} & -\frac{\overline{R}}{L} & 0 & \frac{\Pr}{L} & -I_{\sin} \\ 0 & -\overline{R} & 0 & 0 & 0 & 0 & 0 \\ 0 & 0 & 0 & -\overline{R} & 0 & 0 & 0 \\ \frac{Uc_{\sin}}{\sqrt{U^2c_{\sin}+U^2c_{\cos}}} & 0 & \frac{Uc_{\cos}}{\sqrt{U^2c_{\sin}+U^2c_{\cos}}} & 0 & 0 & 0 & 0 \end{bmatrix} \tag{20}$$

With the following uncertainty block:

$$\Delta=\begin{bmatrix} \delta_R & 0 \\ 0 & \delta_R \end{bmatrix} \tag{21}$$

To design the controller which ensures good tracking and limits the control signals energy we have to solve the mixed sensitivity problem, also called S over KS design. With other words we have to find the controller K which minimizes the sensitivity and the K sensitivity (Gu, 2005).

$$K_{\min}\left\|\begin{matrix}(I+GK)^{-1} \\ K(I+GK)^{-1}\end{matrix}\right\|_{\infty} \tag{22}$$

To point out the significance of the performance requirements over specific frequency ranges weighting functions had been added, which altered controller design requirements as follows:

$$K_{\min}\left\|\begin{matrix}W_p(I+GK)^{-1} \\ W_uK(I+GK)^{-1}\end{matrix}\right\|_{\infty} \tag{23}$$

In this case two weighting functions had been introduced: Wp and Wu.

Wp ensures good disturbance attenuation and has the following form:

$$Wp=\frac{0.05}{10^{-5}s+10^{-7}} \tag{24}$$

The form of Wp was selected so that the singular values of 1/Wp to be above of the singular values of the sensitivity function $(I+GK)^{-1}$ over all frequency ranges(Zhou, 2008).

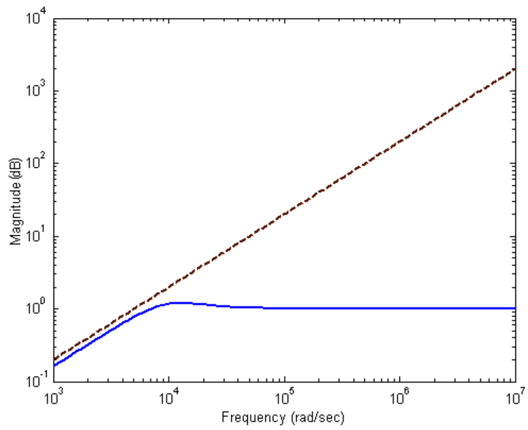

Fig. 11. Singular values of sensitivity and 1/Wp.

The weight function Wu was selected to be a scalar of 0.02.

The closed loop system with weighting functions and uncertainties for which the controller K has to be designed has the following form:

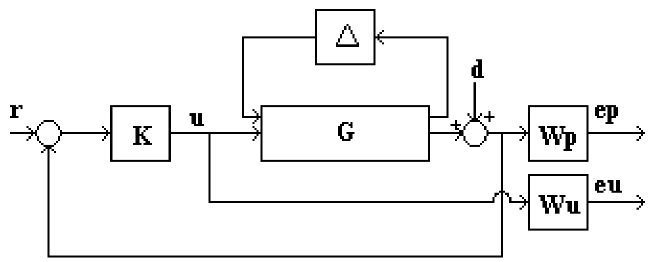

Fig. 12. Closed loop system.

To compute the controller K, the transfer function matrix from disturbance to error had to be extracted:

Were:

$$e=\begin{bmatrix} ep \\ eu \end{bmatrix} \tag{25}$$

By minimizing the H_∞ norm of the system:

$$\begin{bmatrix} Ucs \\ Is \\ Ucc \\ Ic \\ Wps \\ Wp \\ Wu \\ Y+d \end{bmatrix} = \begin{bmatrix} 0 & 1/C & \omega & 0 & 0 & 0 & Uc_{\cos} \\ 1/L & -\bar{R}/L & 0 & \omega & 0 & 0 & Ic \\ -\omega & 0 & 0 & 1/C & 0 & 0 & -Uc_{\sin} \\ 0 & -\omega & 1/L & -\bar{R}/L & 0 & 0 & -Is \\ \frac{Uc_{\sin}}{\sqrt{U^2c_{\sin}+U^2c_{\cos}}}B_{Wp} & 0 & \frac{Uc_{\cos}}{\sqrt{U^2c_{\sin}+U^2c_{\cos}}}B_{Wp} & 0 & A_{Wp} & B_{Wp} & 0 \\ 0 & 0 & 0 & 0 & C_{Wp} & 0 & 0 \\ 0 & 0 & 0 & 0 & 0 & 0 & -Wu \\ \frac{-Uc_{\sin}}{\sqrt{U^2c_{\sin}+U^2c_{\cos}}}B_{Wp} & 0 & \frac{-Uc_{\cos}}{\sqrt{U^2c_{\sin}+U^2c_{\cos}}}B_{Wp} & 0 & 0 & -1 & 0 \end{bmatrix} \cdot \begin{bmatrix} Ucs \\ Is \\ Ucc \\ Ic \\ Wstate \\ d \\ control \end{bmatrix}$$

The following controller resulted:

$$K = \begin{bmatrix} -.17 & -6.31 & 2.43 & 0.52 & -590 & 0 & 0 \\ -0.07 & -1.65 & 0.058 & 0.23 & -146.72 & 0 & 0 \\ 0.02 & 4.67 & -1.65 & -0.09 & 418.47 & 0 & 0 \\ -0.06 & -2.41 & 0.79 & 0.17 & -206.91 & 0 & 0 \\ 0 & 0 & 0 & 0 & 0 & 0 & 0 \\ 0.01 & 0.44 & -0.16 & -0.03 & 39.42 & 0 & 0 \\ 0 & 0 & 0 & 0 & 0 & 0 & -\inf \end{bmatrix} \cdot 10^6 \tag{26}$$

5. PID CONTROLLER FOR THE HEATING INVERTER

The controller for the frequency controlled induction heating inverter was designed using root locus method (Zarnescu, 1999) (Dobra, 2007). To apply the method we determine the transfer function model from the nominal system state space representation, using the (27) formula (Cirtoaje, 2009).

$$H_f(s) = C(sI_4 - A)^{-1}B \tag{27}$$

$$H_f(s) = \frac{1.455\cdot 10^{-11}s^3 + 3.815\cdot 10^{-5}s^2 - 2.654\cdot 10^{-11}s - 4.037\cdot 10^{16}}{s^4 + 2.805\cdot 10^4 s^3 + 3.62\cdot 10^{10}s^2 + 5.05\cdot 10^{14}s + 2.804\cdot 10^{18}} \tag{28}$$

We reduce the order by neglecting the insignificant terms, after we divide all of them by $2.804\cdot 10^{18}$. The plant model obtained is (29). The model is stable, and of minimum phase as shown in figure 13, were we represented the step response for the transfer function model and the simplified transfer function.

$$H_f(s) = \frac{-9.4\cdot 10^{-8}s - 0.014}{1.29\cdot 10^{-8}s^2 + 0.0001801\,s + 1}$$

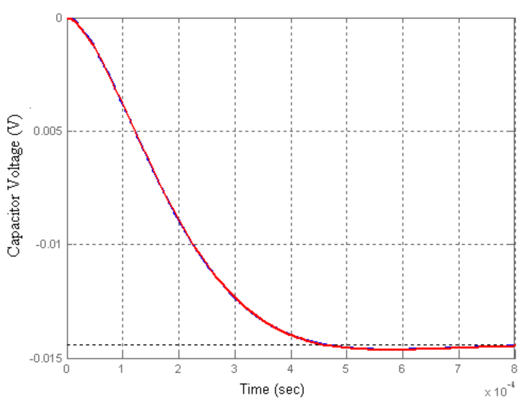

Fig. 13. Step response for high order and reduced system.

The closed loop behaviour is given according with the specification of some performance indices required for the step response. The imposed form for the closed loop transfer function is:

$$H_0(s) = \frac{\omega_n^2}{s^2 + 2\xi\omega_n s + \omega_n^2} \tag{30}$$

The performance requirements for the closed loop system are:

$$\sigma^* = 30\%$$

$$t_r = 1.5 m\sec$$

The damping ratio can be determined from the specified maximum overshoot σ^*.

$$\xi = \frac{|\ln\sigma|}{\sqrt{\pi^2 + (\ln\sigma)^2}}, \sigma \le \sigma^* \tag{31}$$

From the specified maximum settling time the natural frequency is being calculated.

$$\omega_n = \frac{4}{\xi t_r}, t_r \le t_r^* \tag{32}$$

Using formulas (31) and (32) we obtain:

$$\xi = 0.3579$$

$$\omega_n = 7451.8$$

The above values are replaced in equation (30), and we obtain the closed loop transfer function as follows.

$$H_0(s) = \frac{5.553\cdot 10^7}{s^2 + 533s + 5.553\cdot 10^7} \tag{33}$$

To calculate the controller we use the following formula.

$$H_R(s) = \frac{1}{H_f(s)}\cdot\frac{H_0(s)}{1 - H_0(s)} \tag{34}$$

$$H_R(s) = \frac{-7.62\cdot 10^6 - 1.06\cdot 10^{11} - 5.907\cdot 10^{14}}{s^3 + 51.585\cdot 10^5 s^2 + 8.17\cdot 10^8 s} \tag{35}$$

We reduce the controller order by neglecting the smaller coefficient after dividing the transfer function with $5.907 \cdot 10^{14}$.

$$H_R(s) = \frac{-7 - 1.794 \cdot 10^{-4} s - 1}{1.3831 \cdot 10^{-6} s} \quad (36)$$

In the end we obtain the classic PI controller (37).

$$H_R(s) = -129.7086\left(1 + \frac{1}{1.7939 \cdot 10^{-4} s}\right) \quad (37)$$

6. SIMULATION RESULTS

Simulations were made in Matlab for nominal plant and the plant obtained with the resistor variation of ±45%.

The plant nominal values are: R=0.4575 Ω, L=32.6 μH and C=3.6 μF.

Plant responses for a 6V step are presented in figure 14.

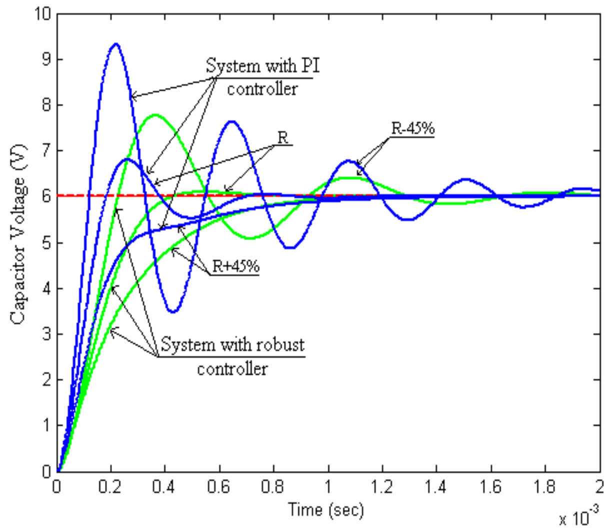

Fig. 14. Step response.

As it can be observe in the figure above the PI controlled inverter has a 58% maximum overshoot and the worst settling time is 2 msec. The robust controlled inverter has a better behaviour with a maximum overshoot of 30% and a settling time of 1.3 msec.

Plant behaviour for a 2V step disturbance is presented in figure 15.

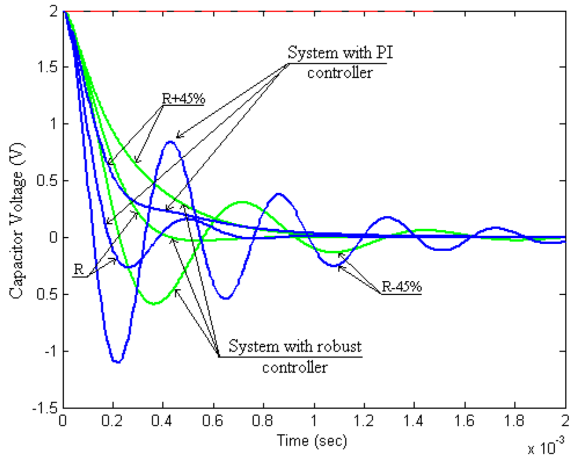

Fig. 15. Disturbance attenuation.

The PI controller rejects the 2V step disturbance in maximum 2 msec while the robust controller rejects the same disturbance in maximum 1.3 msec.

7. CONCLUSIONS

Looking at figure 14 and figure 15 it can be observed that the robust controlled inverter has better performances than the closed loop using classic PI controller obtained with the root locus method. Analyzing the worst scenario with both controllers the robust controlled system has lower overshoot (30%) and faster settling time (1.3 msec). Disturbance attenuation is faster for the robust controller (1.3 msec) than with classic controller (2 msec).

The practical implementation difficulty for the robust controller is the high amount of calculus that has to be solved in each switching period. For the studied inverter the switching period is about 66 μsec. In our days the DSP technology allows us to perform calculus at megahertz frequency, making the practical implementation possible.

To research the practical implementation and inverter performance the PIC32MX360F512L 32 bit microcontroller will be used from Microchip in form of PIC32 starter kit.

ACKNOWLEDGMENT

This paper was supported by the project "Doctoral studies in engineering sciences for developing the knowledge based society-SIDOC", contract no. POSDRU/88/1.5/S/60078, project co-funded from European Social Fund through Sectorial Operational Program Human Resources 2007-2013.

REFERENCES

http://virtual.cvut.cz/dynlabmodules/ihtml/dynlabmodules/syscontrol/node73.html

http://wwwhome.math.utwente.nl/~meinsmag/dmcs/docs/DMCSn2.pdf , page 34 - 38

Cirtoaje, V., Baiesu, A.A., Mihalache, A.S., (2009), *Two controller design procedures using closed-loop pole placement technique,* CEAI, Vol. 11, No. 1, pages 34-42

Damen, A., Weinland, S. (2002). *Robust control*, chapter 7, Eindhoven University of Technology, Eindhoven.

Dede, E.J., Gonzalez, J.V., Linares, J.A., Jordan, J., Ramirez, D., Rueda, P. (1991), 25-kW/50-kHz generator for induction heating, IEEE transactions on industrial electronics, Vol. 38, No. 3, pages 203-209

Dobra, P., Trusca, M., Moga, D., Petreus, D. (2007), *Stability aspects in dc-dc converters using PID controller,* CEAI, Vol. 9, No. 1, pages 33-40

Doyle, J., Glover, K., Khargonekar, P., Francis, B. (1989), *State-space solutions to standard H-2 and H-infinity control problems*, IEEE Trans. Auto. Control, AC-34(8), pages 831-847

Gu, D.W., Petrov, P. Hr., Konstantinov, M.M. (2005). *Robust control design with Matlab*, chapters 4 and 8, Springer-verlag, London.

Iordache, M., Dumitriu, L., (2000), *Teoria moderna a circuitelor electrice* vol. 2, page 28-33., ALL, Bucuresti.

Kazimierczuk, M.K., Czarkowski, D., (1995), Resonant power converters, chapter 6 and 10, John Wiley & Sons Inc, New York

Kelemen, A., Kutasi, N., (2009), *Lyapunov-Based Frequency-Shift Power Control of Induction-Heating Converters with Hybrid Resonant Load,* Acta Universitatis Sapientiae, Electrical and Mechanical Engineering, 1, pages 41-52

Sanchez-Pena, R., Sznaier, M. (1998)., *Robust systems theory and applications,* chapter 6.2 and 11.4, John Wiley & Sons Inc, New York.

Szelitzky, T., Dulf., E.H. (2010), *Advantages of robust control for series loadpulse amplitude modulation induction heating inverters*, Proceedings of 2010 IEEE International Conference on Automation, Quality and Testing, Robotics, Tome I, pages 117-120

Toivonen, H. (1998). *Robust control methods*, chapter 4, Abo Akademi University, Turku Finland.

Tomse, M., Popescu, V., Pasca, S. (2004), *Resonant inverter modelling for induction heating,* Symposium of Electronics and Telecommunications ETC, Timisoara, pages 53-58

Tomse, M., Pasca, S. (2007), *Fuzzy control of resonant inverter for induction heating,* 11th International conference on microwave and high frequency heating, Oradea, pages 136-139

Uchihori, Y., Kawamura, Y., Tokiwa, M., Kim, Y.J., Nakaoka, M. (1995), *New induction heated fluid energy conversion processing appliance incorporating auto-tuning PID control-based PWM resonant IGBT inverter with sensorless power factor correction,* Power Electronics Specialists Conference, vol. 2, pages 1191 - 1197

Zarnescu, H., (1999) *Ingineria reglarii automate II - Proiectarea sistemelor de reglare automata*, page 34 – 38, Targu Mures

Zhou, K. (2008). *Essentials of robust control*, chapter 14.6, Prentice-Hall, New Jersey.